

Catalysis Science & Technology

Accepted Manuscript

This article can be cited before page numbers have been issued, to do this please use: L. Gao, M. Delle Piane, M. Corno, F. Jiang, R. Raja and M. Pera-Titus, *Catal. Sci. Technol.*, 2024, DOI: 10.1039/D3CY01605F.



This is an Accepted Manuscript, which has been through the Royal Society of Chemistry peer review process and has been accepted for publication.

Accepted Manuscripts are published online shortly after acceptance, before technical editing, formatting and proof reading. Using this free service, authors can make their results available to the community, in citable form, before we publish the edited article. We will replace this Accepted Manuscript with the edited and formatted Advance Article as soon as it is available.

You can find more information about Accepted Manuscripts in the [Information for Authors](#).

Please note that technical editing may introduce minor changes to the text and/or graphics, which may alter content. The journal's standard [Terms & Conditions](#) and the [Ethical guidelines](#) still apply. In no event shall the Royal Society of Chemistry be held responsible for any errors or omissions in this Accepted Manuscript or any consequences arising from the use of any information it contains.

ARTICLE

Synthesis of amine derivatives from furoin and furil over Ru/Al₂O₃ catalyst

Li Gao,^a Massimo Delle Piane,^{b†} Marta Corno,^c Fan Jiang,^a Robert Raja^d and M. Pera-Titus^{a,e*}

Received 00th January 20xx,
Accepted 00th January 20xx

DOI: 10.1039/x0xx00000x

The direct/reductive amination of carbohydrate-based furoin and furil with NH₃/H₂ was investigated to access amine derivatives. In the sole presence of NH₃, cyclic amines, i.e. 2,3,5,6-tetra(furan-2-yl)pyrazine and 2,2'-bipyridine-3,3'-diol, were generated as main products from furoin and furil, respectively. Over Ru/Al₂O₃ under NH₃/H₂, 2-amino-1,2-di(furan-2-yl)ethan-1-ol (i.e. alcohol-amine) was generated as main product with 47% yield at 140 °C for 2 h starting from furoin. The catalyst could be recycled for at least three consecutive runs. An alcohol-imine was the main intermediate that underwent tautomerization to alcohol-enamine/keto-amine leading to cyclic by-products by self-condensation. DFT calculations, complementing the experimental observations, provide a detailed molecular-level insight into the reactivity of the alcohol-imine intermediate. Its preferential adsorption on Ru centers *via* the NH group with the OH group pointing away from the surface, directs the reaction pathway towards the formation of alcohol-amine as main product. By combining Ru/Al₂O₃ and a silica-anchored N-heterocyclic carbene (NHC) catalyst, 2-amino-1,2-di(furan-2-yl)ethan-1-ol could be accessed with 42% overall yield in a single reactor.

Introduction

Furfural (FF) is a cheap commercial platform molecule (1.0-1.2 €/kg) that can be prepared at large scale by dehydration of carbohydrates (>200 kT/year).¹ FF can be used as building block for accessing a variety of products and intermediates.^{1c,2} In particular, FF can be converted into amines by reductive amination, which are valuable intermediates to manufacture polymers, surfactants, biologically active molecules and pharmaceuticals (e.g., furosemide).³ The synthesis of furfuryl-amines was investigated from FF and 5-hydroxymethylfurfural

(HMF) by direct/reductive amination over homogeneous and heterogeneous catalysts.⁴ Also, secondary and tertiary tetrahydrofurfurylamines can be accessed with high yield (>90%) from FF over Pd/Al₂O₃ at room temperature and 1 bar H₂.⁵

An upgrading process of FF comprises C-C bond coupling and amination. In this view, it is desirable to design multistep processes with high degree of intensification and high activity/selectivity to the desired amines. One-pot reactions have been reported for the synthesis of furan- and THF-derived amines combining an aldol condensation reaction of FF with ketones, followed by reductive amination with NH₃ and H₂, over a mixture of Amberlyst-26 (A26) and Ru/C or Pd/Al₂O₃ catalysts.⁶ For example, using Pd/Al₂O₃ as catalyst and H₂ (2.0 MPa) as reductant, 98% overall yield of THF-amine was achieved at 120 °C after 20 h.^{6b}

Benzoin condensation is a C-C coupling reaction that can promote the self-condensation of aldehydes using nucleophiles such as cyanides or N-heterocyclic carbenes (NHC) as catalysts.⁷ FF and HMF can self-condense towards 5,5'-dihydroxymethylfuroin (DHMF) derivatives using NHC organo-catalysts.⁸ The reaction mechanism operates *via umpolung condensation* as proposed by Breslow.⁹ In particular, benz-imidazolium (bim) salts with one/two long-chain aliphatic substituents at the N-atoms in the imidazole ring are active catalysts for the reaction.¹⁰ Bim catalysts have been supported over silica and polymers with controlled mesoporosity, affording recyclable heterogeneous catalysts.¹¹ In the presence of base (e.g., 1,8-diazabicyclo-[5.4.0]undec-7-ene, DBU), supported bim catalysts can catalyze the self-condensation of FF into furoin with 96-99% yield over three consecutive runs. Sequential reactions have been developed encompassing furoin derivatives targeting the synthesis of branched alkanes. Furoin/furil intermediates issued from FF can be hydrogenated towards THF-derivatives and subjected to ring opening by hydrodeoxygenation over Pd/C + La(OTf)₃/Eu(OTf)₃ catalysts, accessing C₁₀-C₁₂ diesel fuels.^{8b,12} Furoin/furil intermediates were also employed to prepare C₁₂ biofuels by subsequent esterification and etherification reactions.¹³

Herein we investigated the reactivity of furoin and furil in the direct/reductive amination with NH₃/H₂ over 5%Ru/Al₂O₃. DFT calculations were implemented to rationalize the nature and stability of surface species on Ru(0001) in the presence of adsorbed NH₃ and ad-H, as well as the formation of 2-amino-1,2-di(furan-2-yl)ethan-1-ol (i.e. alcohol-amine) as main product and the alcohol-imine and its tautomers leading to cyclic by-products. We also engineered a single-reactor

^a Eco-Efficient Products and Processes Laboratory (E2P2L), UMI 3464 CNRS-Solvay, 3966 Jin Du Road, Xin Zhuang Ind. Zone, 201108 Shanghai, China.

^b Faculty of Production Engineering and Bremen Center for Computational Materials Science, University of Bremen, Am Fallturm 1, 28359 Bremen, Germany.

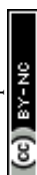
^c Department of Chemistry, University of Torino, Via P. Giuria 7, 10125 Torino, Italy

^d School of Chemistry, University of Southampton, Highfield campus, Southampton SO171BJ, UK

^e Cardiff Catalysis Institute, School of Chemistry, Main Building, Cardiff University, Park Place, Cardiff CF10 3AT, UK, E-mail: peratitusm@cardiff.ac.uk

[†] Current address: Department of Applied Science and Technology, Politecnico di Torino, Corso Duca degli Abruzzi 24, 10129 Torino, Italy

Electronic Supplementary Information (ESI) available: [details of any supplementary information available should be included here]. See DOI: 10.1039/x0xx00000x

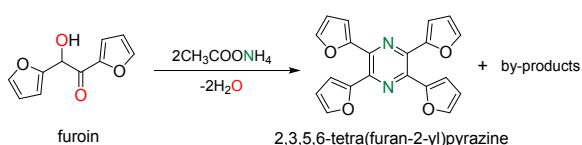


tandem process by combining silica-supported bim to catalyze benzoin condensation (C-C coupling), and 5%Ru/Al₂O₃ to catalyze reductive amination, to access furoin alcohol-amine starting from FF.

Results and Discussion

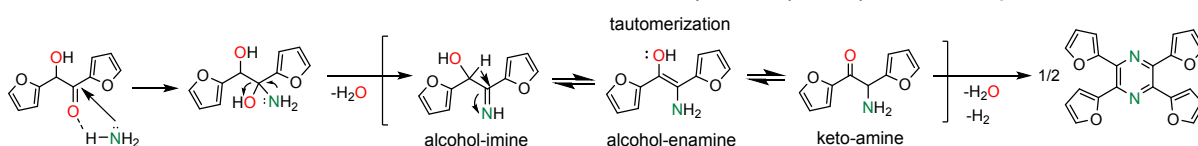
Catalyst-free conversion of furoin / furil under NH₃

Furoin was first reacted with both NH₃ and ammonium acetate as NH₃ surrogate in N,N-dimethylformamide (DMF). 2,3,5,6-Tetra(furan-2-yl)pyrazine is generated as main product at a temperature higher than 130 °C (Scheme 1), which is in accordance with an earlier report.¹⁴ The yield is about 15-18% at full furoin conversion by reacting furoin at 140 °C for 4 h, using 0.06 g of furoin, 6 mL of DMF and 1 g of ammonium acetate (or 0.22 g NH₃). A myriad of minor products is generated with low yield (<5%), including 2-amino-1,2-di(furan-2-yl)ethan-1-ol. The easier operation and higher solubility of ammonium acetate as masked NH₃ reagent compared to gas NH₃ prompted us to use this reagent in the forthcoming experiments.

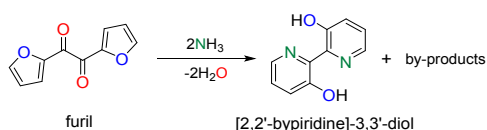


Scheme 1. Catalyst-free furoin amination with NH₃/ammonium acetate.

We explored the effect of the operation variables on the yield of 2,3,5,6-tetra(furan-2-yl)pyrazine at 140 °C for 4 h. Among the solvents tested, DMF, THF and 2-methyl-THF afford a yield of 18-21% (Table S1). The reaction does not proceed in water most likely due to the poor solubility of furoin. We further studied the effect of the temperature using THF while



Scheme 2. Proposed mechanism for 2,3,5,6-tetra(furan-2-yl)pyrazine formation from the reaction of furoin with ammonium acetate / NH₃.



Scheme 3. Catalyst-free furil amination with NH₃.

Furoin and furil amination in the presence of catalyst

With the results above, we studied the reductive amination of furoin and furil with NH₃ and H₂. The catalytic tests were first conducted using furoin at 80 °C and 100 °C in DMF over 5%Pd/Al₂O₃ and 5%Ru/Al₂O₃ catalysts (Fig S1, Fig 1). Pd/Al₂O₃ provides a broad distribution of products, especially at lower temperature (Fig 1A). In contrast, the alcohol-amine is formed as main product over Ru/Al₂O₃ (Fig 1B), as confirmed by GC-MS and ¹H NMR (presence of two doublets centered at 4.7

keeping the other reaction conditions unchanged (Table S2). The yield of 2,3,5,6-tetra(furan-2-yl)pyrazine increases monotonously in the range 130-160 °C up to 30% at full conversion. The highest yield (30%) occurs for an ammonium acetate loading above 0.1 g at 160 °C in THF (Table S3). The yield of 2,3,5,6-tetra(furan-2-yl)pyrazine is 44% at 160 °C for 3 h using dry THF and dry ammonium acetate (Table S4).

A possible reaction mechanism for 2,3,5,6-tetra(furan-2-yl)pyrazine formation by reaction of furoin with ammonium acetate / NH₃ is depicted in Scheme 2. The first step consists of the nucleophilic attack of NH₃ to the carbonyl group of furoin to generate an alcohol-imine intermediate with concomitant release of one water molecule. This intermediate can undergo tautomerization to alcohol-enamine/keto-amine by-products (m/z = 191) that can be hardly distinguished by GC-MS. The self-condensation of the keto-amine, followed by dehydrogenation, results in 2,3,5,6-tetra(furan-2-yl)pyrazine.

Next, we reacted furil with NH₃ in DMF. 2,2'-Bipyridine-3,3'-diol is generated as main product with a yield of 22% at 170 °C after 4 h at full furil conversion (Scheme 3, Table S5). A variety of by-products is generated with low yield (<5%), including 2-amino-1,2-di(furan-2-yl)ethan-1-ol and 1,2-di(furan-2-yl)ethane-1,2-diamine (i.e. diamine). The yield of 2,2'-bipyridine-3,3'-diol increases to 36% at 180 °C, but decreases further to 24% at 200 °C (Table S6). This observation suggests partial product/substrate decomposition at higher temperature. The formation of 2,2'-bipyridine-3,3'-diol can be rationalized on the basis of the mechanism depicted in Scheme 4. Furil reacts fast with NH₃ generating a diimine intermediate. This intermediate is unstable and may be easily activated by a proton in solution favoring ring activation and intramolecular rearrangement leading to pyridine rings. The diimine intermediate can also suffer from reversible polymerization, as earlier observed for diformylfuran upon exposure to NH₃.¹⁵

ppm and 5.4 ppm) (Fig S2). The alcohol-imine and its possible tautomers (keto-amine, alcohol-enamine), and the keto-imine, appear as main by-products. The detection of keto-imine suggests the formation of furil along the reaction from furoin dehydrogenation despite the presence of H₂. Indeed, we confirmed that furil can be generated at room temperature under neat conditions (i.e. without NH₃/H₂) (Fig 1C). Additional peaks are observed at higher temperature (not shown) that can be attributed to cyclic by-products, especially 2,3,5,6-tetra(furan-2-yl)pyrazine, and minor formation of oligomers.

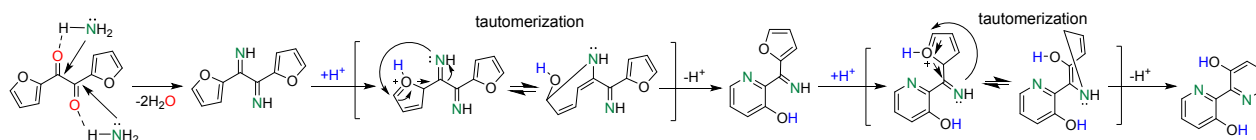
We measured the yield of alcohol-amine from furoin amination over 5%Pd/Al₂O₃, 5%Ru/Al₂O₃, 5%Rh/Al₂O₃ and 5%Pt/Al₂O₃, at 160 °C for 2 h (Table 1). The first three catalysts exhibit poor yield (up to 28%) (entries 1-3), whereas the yield over 5%Ru/Al₂O₃ is the highest (40%) (entry 7) at full furoin conversion. The yield of alcohol-amine is poorly affected by



the Ru loading (entries 4-6) and the type of support (i.e. alumina, silica, carbon) at the same Ru loading (5 wt%) (entries 7-9). The alcohol-imine and its tautomers are generated as

main by-products, as well as 2,3,5,6-tetra(furan-2-yl)pyrazine (not quantified).

DOI: 10.1039/D3CY01605F



Scheme 4. Possible mechanism for 2,2'-bipyridine-3,3'-diol formation from the reaction of furil with NH_3

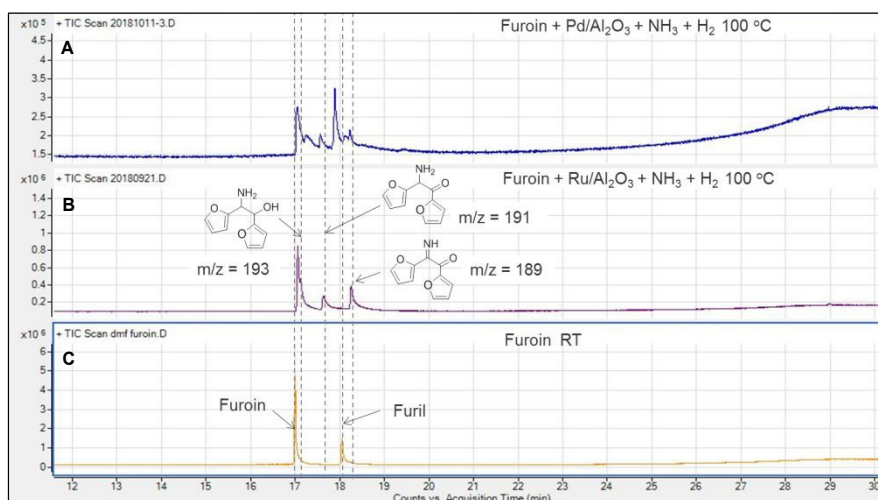


Fig 1. Representative GC plots for furoin amination with NH_3 and H_2 over (A) 5%Pd/ Al_2O_3 , (B) 5%Ru/ Al_2O_3 , and (C) neat conditions (RT) with neither NH_3 nor H_2 . Reaction conditions: furoin (0.12 g, 0.625 mmol), catalyst (24 mg), NH_3 (0.7 g), DMF (2 g), 100 °C, 4.0 MPa H_2 , 2 h. The catalysts were pre-reduced at 200 °C before the reaction.

Table 1. Survey of catalysts for the reductive amination of furoin with NH_3 and H_2 ^[a]

Entry	Catalyst	Yield of alcohol-amine (%)
0	-	0
1	5%Pd/ Al_2O_3	28
2	5%Rh/ Al_2O_3	10
3	5%Pt/ Al_2O_3	14
4	0.1%Ru/ Al_2O_3	30
5	1%Ru/ Al_2O_3	35
6	2%Ru/ Al_2O_3	40
7	5%Ru/ Al_2O_3 (6.7 nm ^[b])	40
8	5%Ru/ SiO_2	35
9	5%Ru/C (2.8 nm ^[b])	40

^[a] Reaction conditions: furoin (60 mg), NH_3 (0.45 g), %Ru/ Al_2O_3 (12 mg), DMF (2 mL), 160 °C, 2 h, H_2 (2.0 MPa). The catalyst was pre-reduced at 200 °C before the reaction. ^[b] Average particle size of Ru nanoparticles measured by HR-TEM

The yield of alcohol-amine increases with the temperature in the range 80-140 °C at 4.0 MPa H_2 pressure with a maximum value of 47%, but decreases slightly further to 40% at 160 °C that we attribute to the formation of oligomers (Fig 2). The yield of alcohol-amine also increases with the H_2 pressure in the range 0.5-4.0 MPa at constant temperature (160 °C) and keeps unchanged beyond 4.0 MPa (Fig 3). The alcohol-imine (and possible tautomers) are generated as main by-products, which can be further hydrogenated to the alcohol-amine product and generate 2,3,5,6-tetra(furan-2-yl)pyrazine and oligomers that were not quantified. However, the keto-imine, which is generated at 80 and 100 °C, vanishes at higher temperature. The catalyst is robust under reaction conditions,

and can be reused for three consecutive catalytic runs with a yield of alcohol-amine in the range 40-45% (Fig 4).

We also studied the reductive amination of furil with NH_3 and H_2 over Ru/ Al_2O_3 . As in the case of furoin, the alcohol-amine is generated as main product with 34% yield together with the diimine and 2,2'-bipyridine-3,3'-diol as main by-products, as well as oligomers. Diamines are generated with less than 5% yield.

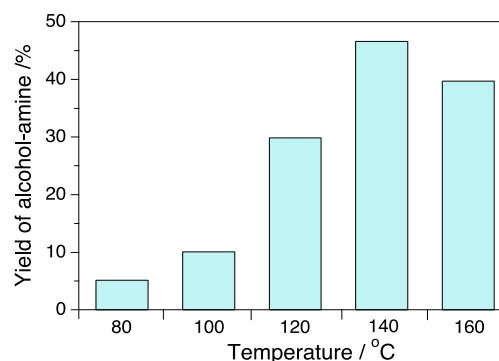


Fig 2. Effect of temperature on furoin amination with NH_3/H_2 over 5%Ru/ Al_2O_3 . Reaction conditions: furoin (60 mg), NH_3 (0.45 g), 5%Ru/ Al_2O_3 (12 mg), DMF (2 mL), 2 h, 2.0 MPa H_2 , catalyst pre-reduced at 200 °C before the reaction. The furoin conversion was complete in all experiments. Alcohol-imine tautomers and 2,3,5,6-tetra(furan-2-yl)pyrazine were generated as main by-products (not quantified).



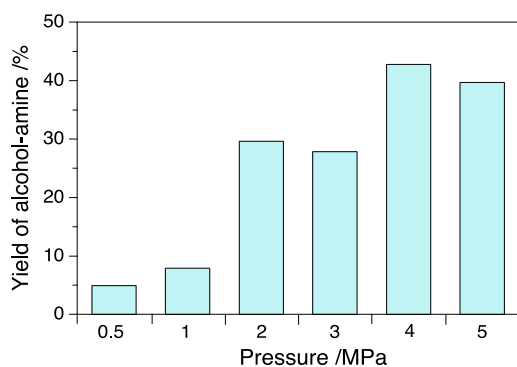


Fig 3. Effect of H₂ pressure on furoin amination with NH₃/H₂ over 5%Ru/Al₂O₃. Reaction conditions: furoin (60 mg), NH₃ (0.45 g), 5%Ru/Al₂O₃ (12 mg), DMF (2 mL), 160 °C, 2 h, catalyst pre-reduced at 200 °C before the reaction. The furoin conversion was complete in all experiments. Alcohol-imine tautomers and 2,3,5,6-tetra(furan-2-yl)pyrazine were generated as main by-products (not quantified).

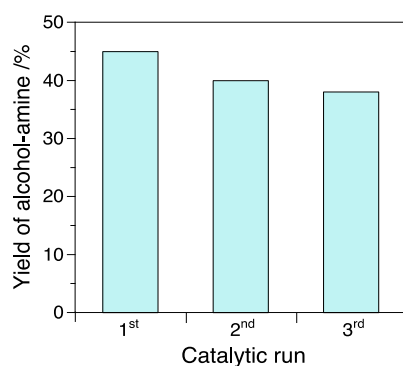


Fig 4. Catalyst recycling and reuse for experiments carried out over 5%Ru/Al₂O₃. Reaction condition: 60 mg furoin, 0.45 g NH₃, 0.012 g 5% Ru/Al₂O₃, 2 mL DMF, 2 h, 4.0 MPa H₂, catalyst pre-reduced at 200 °C before the reaction.

Understanding furoin amination over 5%Ru/Al₂O₃

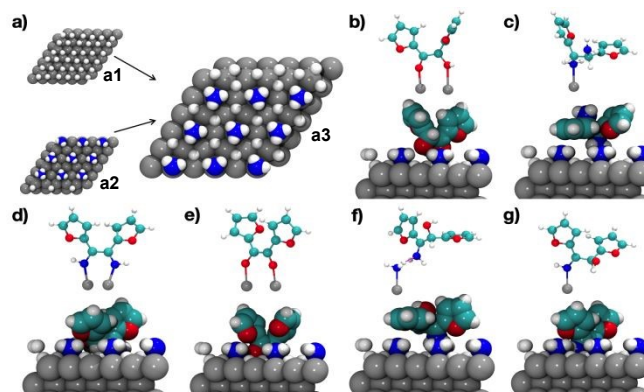
The results above point out the preferential formation of the alcohol-amine product over Ru/Al₂O₃ at 140 °C and 2.0 MPa H₂ pressure starting from furoin, with ketone-amine/alcohol-imine as main intermediates. To rationalize the formation of the alcohol-amine and cyclic by-products, we computed the adsorption configurations and energies of the reactants (furoin, furil), end products (alcohol-amine, diamine) and possible intermediates (alcohol-imine + tautomers, diimine). The calculations were carried out both on a reduced, bare reduced Ru(0001) surface and on a reduced Ru(0001) surface covered with NH₃ and ad-H, at the DFT-PBE level (see ESI for computational details).

Table 2 lists the adsorption energies for the optimized configurations of the reactants, products and intermediates on bare and ad-H/NH₃-covered Ru(0001). For adsorbed furoin (entries 1-4), four configurations were probed on the bare Ru(0001) interacting *via* (**Scheme 5**): i) C=O group, ii) OH group, iii) both C=O and OH groups, and iv) furan rings. The most stable configuration, i.e. iii), corresponds to a bidentate binding mode with C=O showing the shortest Ru-O distance. The adsorption energy on bare Ru(0001) (-156 kJ·mol⁻¹) (entry

4) is almost twice the sum of the energies for monodentate adsorption *via* C=O (i) and OH (ii) groups, i.e. -59 and -37 kJ·mol⁻¹, respectively (entries 1-2). No stable configuration occurs *via* furan rings as inferred from the positive adsorption energy (+14 kJ·mol⁻¹) (entry 3).

Table 2. Energy of adsorption (ΔE_{ads} , kJ·mol⁻¹) of reactants, products and intermediates for most stable configurations on bare Ru(0001) and effect of coverage by NH₃ and ad-H^[a]

Entry	Molecule	Interacting groups	ΔE_{ads} @ bare Ru(0001)	ΔE_{ads} @ ad-H and NH ₃ Ru(0001)
1	Furoin	C=O	-59	-
2	Furoin	OH	-37	-
3	Furoin	Furan rings	+14	-
4	Furoin	C=O+OH	-156	-74
5	Furil	C=O + C=O	-115	-107
6	Alcohol-amine	NH ₂	-189	-36
7	Diamine	NH ₂	-91	-24
8	Diimine	NH + NH	-252	-185
9	Alcohol-imine	NH	-92	-31
10	Alcohol enamine	NH ₂	-45	-12
11	Keto-amine	NH ₂	-67	-23



Scheme 5. (a) H₂ and NH₃ coverage and co-coverage on Ru(0001) (a1-a3), and most stable surface configurations for (b) furoin, (c) diamine, (d) diimine, (e) furil, (f) alcohol-amine and (g) alcohol-imine, represented both as balls-and-stick representations of the interactions

Few studies describe the atomistic details of H₂ and NH₃ co-adsorption on Ru(0001).¹⁶ H₂ and NH₃ are known to occupy different sites on the Ru(0001) surface, so that ad-H atoms can influence the adsorption pattern of NH₃ on Ru(0001).¹⁶ Since ad-H atoms occupy mainly fcc sites,¹⁷ we simulated the dissociative H₂ chemisorption on fcc sites and NH₃ adsorption on adjacent top sites. First, we simulated a full monolayer of ad-H on fcc sites without NH₃ (**Scheme 5a1**). The adsorption energy is -111 kJ·mol⁻¹ and keeps unchanged when implicit solvation by DMF is included (-112 kJ·mol⁻¹). Next, we simulated NH₃ chemisorption on only 25% of available top sites to take into account steric constraints (**Scheme 5a2**). Also, we assumed that no NH₃ dissociation occurs at the reaction temperature (up to 160 °C) given its high activation energy (>100 kJ·mol⁻¹),¹⁸ and that adsorbed NH₃ is known to keep undissociated in the presence of ad-H species below 170 °C.^{17,19} The adsorption energy of NH₃ is -75 kJ·mol⁻¹ with limited stabilizing effect of DMF (-5 kJ·mol⁻¹), which agrees well an earlier report.²⁰ The average N-Ru distance is 2.2 Å that is similar to the distance measured for diamine and diimine derivatives. We also computed H₂ and NH₃ co-adsorption on



Ru(0001) (**Scheme 5a3**). After geometry optimization, half of ad-H atoms move to neighboring hcp sites with a hexagonal arrangement around each adsorbed NH_3 molecule. The adsorption energy is $-101 \text{ kJ}\cdot\text{mol}^{-1}$ ($-104 \text{ kJ}\cdot\text{mol}^{-1}$ in DMF).

Using the optimized NH_3 - and ad-H-covered Ru(0001) surface, we simulated the adsorption of furoin/furil, products and intermediates, and recomputed the adsorption energies (**Scheme 5b-g**, **Table 2**). As a rule, although adsorption energies can show variations when different NH_3 and ad-H coverages are considered, the primary effect on the relative stability of the different species and their orientation is expected to be poorly affected.²¹ With these considerations, all adsorption energies are lower on the NH_3 - and ad-H-covered Ru(0001) surface than on bare Ru(0001). However, the relative stability between furoin, diamine and diimine is preserved. Furil exhibits stronger adsorption than furoin ($-107 \text{ kJ}\cdot\text{mol}^{-1}$ vs. $-74 \text{ kJ}\cdot\text{mol}^{-1}$, compare entries 5 and 4), since the C=O–Ru interaction is kept when NH_3 covers the surface (**Scheme 5e**). In contrast, in the case of furoin, NH_3 bridges the interaction between the OH group and the Ru(0001) surface via H-bonding (**Scheme 5b**), resulting in lower stability.

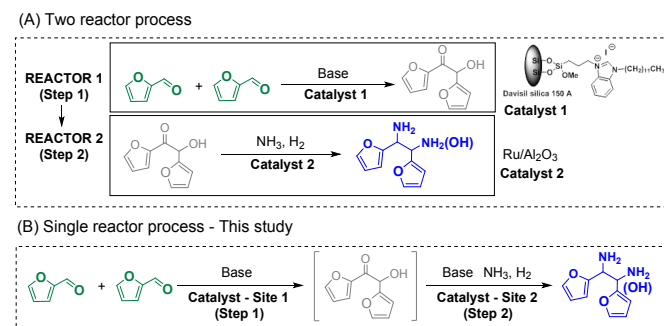
We also investigated the relative stability of the alcohol-imine and its two tautomers on Ru(0001) in the presence of adsorbed NH_3 and ad-H species. The alcohol-imine interacts preferentially with Ru(0001) via the NH group (**Scheme 5g**), but the adsorption energy is lower compared to the value on the bare surface (-31 vs. $-92 \text{ kJ}\cdot\text{mol}^{-1}$, entry 9) due to steric hindrance. The alcohol-imine is $-19 \text{ kJ}\cdot\text{mol}^{-1}$ more stable than the alcohol-enamine and $-8 \text{ kJ}\cdot\text{mol}^{-1}$ more stable than the keto-amine tautomer over NH_3 and ad-H-covered Ru(0001) (entries 10–11) (see also **Fig S3**). This relative stability opposes that observed in bulk solution, where the keto-enamine is the most stable tautomer being $45 \text{ kJ}\cdot\text{mol}^{-1}$ more stable than the alcohol-imine and $27 \text{ kJ}\cdot\text{mol}^{-1}$ less stable than the keto-amine.

This body of results points out that the alcohol-imine is a likely intermediate responsible for the formation of the alcohol-amine over Ru(0001). The weak adsorption of the alcohol-imine and its tautomers over Ru(0001) can favor its desorption from the catalyst and the further formation of 2,3,5,6-tetra(furan-2-yl)pyrazine among other cyclic by-products in bulk solution competing with the alcohol-amine proceeding over the catalyst. Besides, preferential interaction of NH or NH_2 groups of the alcohol-imine and keto-amine, respectively, on Ru(0001) discourages the formation of the diimine and amine-imine intermediates, and in turn hinders diamine formation. This selectivity shortcoming has also been observed in the amination of isosorbide with NH_3 and H_2 , where the *exo*-OH group exhibits much lower reactivity than the *endo*-OH group, resulting in the formation of amino-alcohols with different stereochemistry as main products with small amounts of diamines.^{18,50}

Single-reactor tandem benzoin condensation + reductive amination process

With the results above, we investigated the credentials of a tandem reaction for the synthesis of the alcohol-amine starting from FF by combining supported bim-silica³⁸ and $\text{Ru}/\text{Al}_2\text{O}_3$ catalysts in a single reactor (**Scheme 6**). In this test, both catalysts were loaded in the reactor together with DMF,

FF and DBU to activate bim. First, the benzoin condensation reaction was carried out at 30°C for 20 h. Subsequently, NH_3 and H_2 were added, and the amination reaction was carried out at 140°C for 2 h. The results clearly show the formation of the alcohol-amine product (**Fig 5**) with 42% overall yield.



Scheme 6. Two-reactor vs. single reactor tandem process for the synthesis of hydrogenated derivatives from FF.

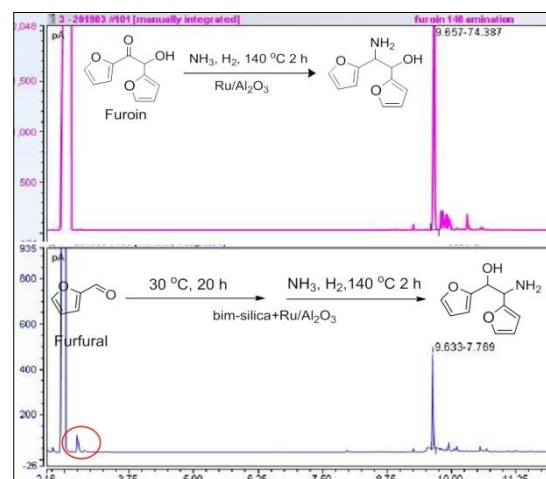


Fig 5. Representative GC plots of the reaction system after the amination reaction of furoin with NH_3 and H_2 over (A) $\text{Ru}/\text{Al}_2\text{O}_3$ and (B) bim-silica + $\text{Ru}/\text{Al}_2\text{O}_3$ in the single-reactor tandem process. Reaction conditions: (top) furoin (0.12 g, 0.625 mmol), catalyst (24 mg), DMF (2 g), NH_3 (0.7 g), 140°C , 4.0 MPa H_2 , 2 h, catalyst pre-reduced at 200°C ; (bottom) (1) Benzoin condensation: FF (0.096 g, 1 mmol), DBU (26 mg, 0.17 mmol), bim-silica (0.16 g), catalyst (24 mg), DMF (2 g), 30°C , 20 h, 5% $\text{Ru}/\text{Al}_2\text{O}_3$ catalyst pre-reduced at 200°C ; (2) Reductive amination: 0.7 g NH_3 , 4.0 MPa H_2 , 140°C , 2 h.

To assess the stability of bim-silica in the presence of NH_3 and H_2 , the catalyst was extracted from the reaction system after the tandem reaction, washed with HCl and DMF and retested in the benzoin condensation of FF. The catalyst was found to be fully active (see chromatogram in **Fig S4**), pointing out that the bim moiety is not detached from the support during the tandem reaction. TG analyses on the fresh and spent bim-silica catalysts confirm the stability of bim-silica during the tandem reaction (**Fig S5**).

Conclusions

Along this study, we studied the direct/reductive amination of furoin and furil with NH_3 and H_2 . Without catalyst, furoin



reacts with either NH₃ or ammonium acetate to generate 2,3,5,6-tetra(furan-2-yl)pyrazine with 39% yield. Furil also reacts with NH₃ to generate 2,2'-bipyridine-3,3'-diol with 44% yield. When Ru/Al₂O₃ and H₂ are added to the reaction system, furin and furil generate 2-amino-1,2-di(furan-2-yl)ethan-1-ol (alcohol-amine) as main product with 47% and 34% yield, respectively, at 140 °C for 2 h. DFT simulations underscored the significance of the unique adsorption orientation of these intermediates on Ru/Al₂O₃, with the NH group in proximity to Ru centers and the OH group oriented away from the surface. This orientation, as revealed by our computational analysis, plays a pivotal role in guiding the reaction towards the formation of alcohol-amine, corroborating the experimentally observed product distribution. The alcohol-imine exhibits weak adsorption on ad-H/NH₃-covered Ru, allowing the formation of 2,3,5,6-tetra(furan-2-yl)pyrazine in solution competing with alcohol-amine formation on Ru. By combining Ru/Al₂O₃ and a silica-anchored N-hetero-cyclic carbene (NHC) catalyst, 2-amino-1,2-di(furan-2-yl)ethan-1-ol could be accessed with 42% overall yield in a single reactor.

Author Contributions

LG: Experimental data acquisition, data curation, formal analysis, writing original draft; MDP & MC: DFT calculation, data curation, formal analysis, writing original draft; FJ: Investigation, formal analysis, supervision; RR: formal analysis, visualization; MPT: conceptualization, funding acquisition, resources, supervision, validation, visualization, writing – review & editing.

Conflicts of interest

There are no conflicts to declare.

Acknowledgements

This project has received funding from the European Union's Horizon 2020 research and innovation program under grant agreement N. 720783-MULTI2HYCAT. MDP acknowledges the computational resources of the Bremen Center for Computational Material Science (BCCMS), University of Bremen, Germany.

References

- (a) R. Mariscal, P. Maireles-Torres, M. Ojeda, I. Sádaba and M. López Granados, *Energy Environ. Sci.*, 2016, **9**, 1144; (b) X. Li, P. Jia and T. Wang, *ACS Catal.*, 2016, **6**, 7621; (c) J.-P. Lange, E. van der Heide, J. van Buijtenen and R. Price, *ChemSusChem*, 2012, **5**, 150.
- (a) J. Thoen and R. Busch, *Industrial Chemicals from Biomass – Industrial Concepts*, in: *Biorefineries-Industrial Processes and Products: Status Quo and Future Directions*, ed B. Kamm, P. R. Gruber and M. Kamm, chapter 12, Wiley, 2005, pp 347; (b) G. W. Huber, J. N. Chheda, C. J. Barrett and J. A. Dumesic, *Science*, 2005, **308**, 1446; (c) J. Q. Bond, A. A. Upadhye, H. Olcay, G. A. Tompsett, J. Jae, R. Xing, D. M. Alonso, D. Wang, T. Zhang, R. Kumar, A. Foster, S. M. Sen, C. T. Maravelias, R. Malina, S. R. H. Barrett, R. Lobo, C. E. Wyman, J. A. Dumesic and G. W. Huber, *Energy Environ. Sci.*, 2014, **7**, 1500-1523; (d) M. J. Climent, A. Corma and S. Iborra, *Green Chem.*, 2014, **16**, 516; (e) K. Yan, G. Wu, T. Lafleur and C. Jarvis, *Renew. Sust. Energy Rev.*, 2014, **38**, 663. DOI: 10.1039/D3CY01605F
- (a) Q. Girka, N. Hausser, B. Estrine, N. Hoffmann, J. Le Bras, S. Marinkovic and J. Muzart, *Green Chem.*, 2017, **19**, 4074; (b) M. Pelckmans, T. Renders, S. Van de Vyver and B. F. Sels, *Green Chem.*, 2017, **19**, 5303; (c) A. Velty, S. Iborra and A. Corma, *ChemSusChem*, 2022, **15**, e202200181.
- (a) J. J. Martínez, E. Nope, H. Rojas, M. H. Brijaldo, F. Passos and G. Romanelli, *J. Mol. Catal. A: Chem.*, 2014, **392**, 235; (b) S. Nishimura, K. Mizuhori and K. Ebitani, *Res. Chem. Intermed.*, 2016, **42**, 19; (c) M. Chatterjee, T. Ishizaka and H. Kawanami, *Green Chem.*, 2016, **18**, 487; (d) T. Komanoya, T. Kinemura, Y. Kita, K. Kamata and M. Hara, *J. Am. Chem. Soc.*, 2017, **139**, 11493; (e) A. Dunbabin, F. Subrizi, J. M. Ward, T. D. Sheppard and H. C. Hailes, *Green Chem.*, 2017, **19**, 397; (f) J. A. T. Caetano and A. C. Fernandes, *Green Chem.*, 2018, **20**, 2494; (g) D. Chandra, Y. Inoue, M. Sasase, M. Kitano, A. Bhaumik, K. Kamata, H. Hosono and M. Hara, *Chem. Sci.*, 2018, **9**, 5949; (h) Z. Kuo, C. Bixian, Z. Xiaoting, K. Shimin, X. Yongjun and W. Jinjia, *ChemCatChem*, 2019, **11**, 5562; (i) D. Deng, Y. Kita, K. Kamata and M. Hara, *ACS Sust. Chem. Eng.*, 2019, **7**, 4692; (j) J. He, L. Chen, S. Liu, K. Song, S. Yang and A. Riisager, *Green Chem.*, 2020, **22**, 6714; (k) K. Saini, S. Kumar, H. Li, S. A. Babu and S. Saravanamurugan, *ChemSusChem*, 2022, **15**, e202200107; (l) C. C. Truong, D. K. Mishra and Y-W. Suh, *ChemSusChem*, 2023, **16**, e202201846.
- S. Jiang, E. Muller, F. Jérôme, M. Pera-Titus and K. De Oliveira Vigier, *Green Chem.*, 2020, **22**, 1832.
- (a) S. Jiang, C. Ma, E. Muller, M. Pera-Titus, F. Jérôme and K. De Oliveira Vigier, *ACS Catal.*, 2019, **10**, 8893; (b) S. Jiang, E. Muller, M. Pera-Titus, F. Jérôme and K. De Oliveira Vigier, *ChemSusChem*, 2020, **13**, 1699.
- (a) D. Enders, O. Niemeier and A. Henseler, *Chem. Rev.*, 2007, **107**, 5606; (b) R. S. Menon, A. T. Biju and V. Nair, *Beilstein J. Org. Chem.*, 2016, **12**, 444.
- (a) D. Liu, Y. Zhang and E. Y-X. Chen, *Green Chem.*, 2012, **14**, 2738; (b) D. Liu and E. Y-X. Chen, *ChemSusChem*, 2013, **6**, 2236; (c) H. Zang and E. Y-X. Chen, *Int. J. Mol. Sci.*, 2016, **16**, 7143; (d) J. Li, B. Wang, Y. Dou and Y. Yang, *RSC Adv.* 2019, **9**, 10825.
- (a) R. Breslow, *J. Am. Chem. Soc.*, 1957, **79**, 1762; (b) R. Breslow, *J. Am. Chem. Soc.*, 1958, **80**, 3719.
- (a) K-I. Iwamoto, H. Kimura, M. Oike and M. Sato, *Org. Biomol. Chem.*, 2008, **6**, 912; (b) K-I. Iwamoto, M. Hamaya, N. Hashimoto, H. Kimura, Y. Suzuki and M. Sato, *Tetrahedron Lett.*, 2006, **47**, 7175.
- (a) L. Wang and E. Y.-X. Chen, *ACS Catal.*, 2015, **5**, 6907; (b) J. Wilson and E. Y.-X. Chen, *ACS Sust. Chem. Eng.*, 2016, **4**, 4927; (c) E. Y-X. Chen, L. Wang and Y. Eguchi, US 0,346,774 A1, 2016; (d) I. Miletto, M. Meazza, G. Paul, M. Cossi, E. Gianotti, L. Marchese, R. Rios, M. Pera-Titus and R. Raja, *Chem. Eur. J.*, 2022, **28**, e202202771.
- (a) D. Liu and E. Y-X. Chen, *ChemSusChem*, 2013, **6**, 2236; (b) D. J. Liu and E. Y-X. Chen, *ACS Catal.*, 2014, **4**, 1302; (c) J. Keskinvalli, P. Wrigstedt, K. Lagerblom and T. Repo, *Appl. Catal. A: Gen.*, 2017, **534**, 40.
- E. Y-X. Chen and D. Liu, US 9,469,626 B2, 2016.
- S. Wang, Q. Gu, X. Chen, T. Zhao and Y. Zhang, *Eur. J. Chem.*, 2011, **2**, 173-177.
- N-T. Le, A. Byun, Y. Han, K-I. Lee and H. Kim, *Green Sust. Chem.*, 2015, **5**, 115-127.
- L. R. Danielson, M. J. Dresser, E. E. Donaldson and J. T. Dickinson, *Surf. Sci.*, 1978, **71**, 599.
- I. M. Ciobîcă, F. Frechard, R. A. van Santen, A. W. Kleyn and J. Hafner, *J. Phys. Chem. B*, 2000, **104**, 3364.
- H. Hu, M. A. Ramzan, R. Wischert, F. Jérôme, C. Michel, K. de Oliveira Vigier and M. Pera-Titus, *ACS Sust. Chem. Eng.*, 2023, **11**, 8229.



- 19 (a) H. Mortensen, L. Diekhöner, A. Baurichter, E. Jensen and A. C. Luntz, *J. Chem. Phys.*, 2000, **113**, 6882.
- 20 X. Hu, M. Yang, D. Xie and H. Guo, *J. Chem. Phys.*, 2018, **149**, 044703.
- 21 N. Gerrits and G-J. Kroes, *J. Phys. Chem. C*, 2019, **123**, 28291.
- 22 R. Pfützenreuter and M. Rose, *ChemCatChem.*, 2016, **8**, 251.

View Article Online
DOI: 10.1039/D3CY01605F

Open Access Article. Published on 19 March 2024. Downloaded on 3/20/2024 3:36:48 PM.
This article is licensed under a Creative Commons Attribution-NonCommercial 3.0 Unported Licence.

